Journal of Engineering Physics and Thermophysics, Vol. 82, No. 2, 2009

SIMULATION AND NUMERICAL INVESTIGATIONS OF THE KINETICS OF ATMOSPHERIC AEROSOL DROPLETS IN THE WAKE BEHIND A FLAT PLATE

A. G. Zdor

UDC 532.529

Within the framework of the physicomathematical model of evolution of a polydisperse condensate, numerical investigations of the kinetics of atmospheric aerosol droplets in a supersonic two-phase flow past a flat plate were carried out. The gas flow was described by the Reynolds equations with the use of the two-parameter turbulence model. In view of the smallness of the condensate mass fraction in the incoming flow, the inverse effect of the dispersed phase on the gas was not considered. For various regimes of exposure to a flow, the characteristic features of the spatial distribution of the main parameters of the condensate fractions have been studied: the number densities, radii, temperatures, and averaged velocities of microdrops. The dependence of the dispersed phase dynamics on the Mach number and the incoming flow angle of attack has been investigated and the influence of the allowance for the processes of coagulation/fragmentation on the mass spectrum of droplets is shown.

Keywords: *supersonic two-phase flow, polydisperse condensate, turbulent pulsations.*

In studying multiphase turbulent flows one has to consider a large number of various physical processes: heat- and mass exchange of a dispersed phase with a carrying gas, fragmentation of droplets under the action of aerodynamic forces, their coagulation/fragmentation in mutual collisions. Each of these processes is an individual topic for investigations and is determined by a number of parameters of the surrounding gas, dispersed phase, as well as by dimensionless numbers. Even though many of them have been studied and described in detail, because of the strong inhomogeneity of the flows considered it turns out very difficult to predict the dominant process at the given spatial-temporal point. It is also necessary to take into account the possible velocity and temperature nonequilibrium state of droplets of different fractions among themselves and with a carrying medium. Therefore it is of interest to carry out a numerical analysis on the basis of complex, synthetic models of the dynamics of multiphase flows, where all of the above-mentioned phenomena are taken into account.

In this work, numerical investigations of the dynamics and changes in the dispersity of water condensate droplets in the wake behind a model configuration of a high-speed flying vehicle are carried out. The aim of the work is to test the model of the dynamics of a two-phase polydisperse flow with the aid of numerical algorithms that make it possible to carry out calculations in a wide range of parameters. Computations were performed in a geometrically simple two-dimensional statement: the flow past a flat plate of small thickness and of downstream finite length located at an angle of attack to the incoming flow. It was assumed that droplets of pure water in the composition of the aerosol of the upper atmospheric layers are in a supercooled state and, while interacting with gasdynamic inhomogeneities of the flow, they participate in a number of physical processes described in detail in [1–4]. The content of the dispersed phase "at infinity" (the ratio of the mass concentration of condensate to the gas density) was taken small, therefore the inverse effect of the aerosol on the gas was not taken into account, and the numerical analysis was carried out in two steps. First, only the gas flow past the plate was considered without allowance for the dispersed phase, and then an atmospheric aerosol was superposed against this background.

A viscous heat conducting perfect gas flow (at $\gamma \approx 1.4$) past a thin flat plate (downstream length 10 m and thickness 6 cm) was considered under the conditions corresponding to a flight in the Earth's atmosphere at an altitude of approximately 10 km at angles of attack 10^{o} and 15^{o} for Mach numbers of the incoming flow M = 2 and 4. A

N. E. Zhukovskii Central Aero-Hydrodynamics Institute, 1 Zhukovskii Str., Zhukovskii, Moscow District, 140160, Russia. Translated from Inzhenerno-Fizicheskii Zhurnal, Vol. 82, No. 2, pp. 331–341, March–April, 2009. Original article submitted November 5, 2008.

two-parameter model was used to describe turbulence [5]. The numerical solution of full nonstationary Reynolds equations was performed by the method of "large particles" [6]. In the zones of oblique shocks and fans of rarefaction waves the results of calculations are in good qualitative agreement with the well-known classical solutions of the problems of an ideal gas flow past thin bodies [7].

In order to describe the dynamics of a condensate, a model of a polydisperse aerosol was used [2–4] that takes into account the fragmentation and coagulation of particles, the influence of turbulent pulsations on the frequency of collisions of droplets and their diffusional displacement, momentum transfer, and heat and mass exchange (just as between fractions, so with a carrying gas). Within the framework of the hydrodynamic model adopted, a two-phase system was represented as a multicomponent continuous medium (three fractions were considered in calculations). It was assumed that all the particles of the given fraction were spherical and that at a fixed spatial–temporal point they had identical velocities, radii, and temperatures; moreover, these values may differ for different fractions. Thus, each fraction at the given point of space and at a given instant of time was characterized by a set of parameters: by the number density and mass concentration of particles, vector of their averaged velocity, mean-bulk temperature of the droplets of a fraction, and by their radius.

In the given model of the dynamics of a polydisperse aerosol mass- and heat exchange of fractions with the carrier gas is admitted. It was assumed that the temperature of each particle was constant over its volume and coincident with its average surface temperature. For a continuous regime of flow around particles, when mass and heat fluxes to the droplet surface are due to diffusion and heat conduction, the total heat flux q_s^{c} and the rate of change in the droplet mass m_s^{c} in the assumption of the exponential dependence of the dynamic viscosity of the gas on temperature $\mu_{\mathrm{m}}(T) = \text{const}\ T^{\omega}$ are described in detail in [1]. In order to calculate m_s^{c} and q_s^{c}, gas parameters that correspond to the conditions of adiabatic recovery are used. In calculations the recovery factor was assumed equal to unity for several reasons. First, it is proportional to the square root of the Prandtl number ($\mathrm{Pr} \approx 0.74$) which itself is close to unity; second, as calculations showed, the Mach numbers of flow around droplets of all fractions do not exceed the value $\mathrm{M} \approx 0.8$. Therefore the errors introduced by the assumption made are rather small and lie within the framework of the errors of calculation. The flows considered are extremely inhomogeneous, and for this reason the fixed particle moving along the trajectory may find itself under different conditions that determine the character of the processes of its heat- and mass exchange with the carrier medium. On the basis of the data of works [1, 8], for large Knudsen numbers of the flow around a droplet for total mass and heat fluxes to its surface, dependences that take into account the velocity slip of phases were used.

For a spherical particle exposed to a gas flow, the force acting on it consists of several terms. Only one term was considered in the calculations, viz., the force of aerodynamic resistance, for which the following expression was used:

$$\mathbf{F}_s = 0.5\pi a_s^2 \rho C_D \left|\mathbf{u} - \mathbf{v}_s\right| (\mathbf{u} - \mathbf{v}_s) .$$

In the continuous case, a three-term approximation of the standard curve of the resistance coefficient was used with a correction factor that describes its dependence on the Mach number [1, 9]. In the presence of the difference between the temperatures of droplets and a carrying gas it is also necessary to introduce corrections for the resistance coefficient. The expression used for C_D^{c} in calculations is described in detail in [1]. The resistance coefficient of the condensate particles C_D^{r} for a free-molecular flow around them with allowance for the processes of mass transfer and velocity slip was modeled on the basis of the data of [1, 8].

Of great interest is the interpolation of expressions for mass- and heat fluxes and for the coefficient of aerodynamic resistance obtained for the limiting cases of continuous and free-molecular regimes of flow around particles at intermediate values of the Knudsen number. With the aim of decreasing the expenditures of machine time, preference was given to simple variants of interpolation. These requirements of simplicity and adequacy are satisfied, e.g., by formulas of the type of "parallel conductivities" verified under the conditions of subsonic flow around droplets [1]: $\Psi = \Psi^{\mathrm{r}}\Psi^{\mathrm{s}}/(\Psi^{\mathrm{r}} + \Psi^{\mathrm{s}}),\ \Psi \in \{\dot{m}, q, C_D\}$.

To model the processes of coagulation [2–4], the discrete changes in the mass of particles on collisions were conventionally replaced by continuous ones, which leads to asymmetry in the description of interactions of the given fraction with droplets of larger and smaller sizes. It was assumed that particles preserve their affinity to the given fraction

on collisions with smaller particles (projectiles) and leave it on collisions with larger ones (targets); in other words, in the former case the mass is affected, and in the latter case their number. Moreover, it was admitted that a certain portion of the substance returned to the fraction of projectiles in the form of incipient droplets — fragments. Within the framework of the adopted locally monodisperse model of fragmentation in mutual collisions, complex mass, velocity, and temperature spectra of the fragments and targets were replaced by simplified ones. It was assumed that all the fragments formed had the radius of the projectile, with their initial velocities and temperatures coinciding with analogous parameters of the target. The intensity of the fragmentation of the latter was characterized by a semiempirical coefficient of coagulation/fragmentation Φ_{js} (here j is the fraction of projectiles, and s of targets). In [4], interpolation dependences of Φ_{js} on the conditions of collision described in terms of the Reynolds and Laplace numbers are given.

In simulation of the coagulation processes, of importance are the average relative velocities of colliding particles:

$$|\Delta \mathbf{v}_{js}| = \left\{ |\mathbf{v}_j - \mathbf{v}_s|^2 + |\Delta \mathbf{v}_{js}^{\text{rand}}|^2 \right\}^{0.5}.$$

These quantities depend on both the averaged velocities of the fractions $\mathbf{v}_j$ and $\mathbf{v}_s$ and their stochastic components $|\Delta \mathbf{v}_{js}^{\text{rand}}| = |\Delta \mathbf{v}_{js}^{\text{tur}}| + |\Delta \mathbf{v}_{js}^{\text{Br}}|$ that are attributable to the involvement of droplets in turbulent motion of the carrying gas (the first term) and in the Brownian movement (of importance for fine particles) [2]. In the case of a continuous flow around particles, on the basis of the data of [2], it is adopted that $|\Delta \mathbf{v}_{js}^{\text{Br}}| = 2k_{\text{B}}T/(3\pi a_j a_s \mu_{\text{m}}(T))$. Investigation of the interaction of droplets with turbulent pulsations of the flow required a separate consideration. This interaction is one of the reasons for mutual collisions of particles, and also for their diffusive motion. In the work, the results of investigation of the parameters of the relative motion of droplets were used on the basis of the statistical approach [10–12] and the simple approximating relations that follow from them and that are convenient for application in numerical algorithms. The three-dimensional spectrum of turbulence was modeled by means of joining the von Karman and Pao approximations [13]. With this spectrum being taken into account, rigorous results were obtained for the functions that describe the involvement of particles in pulsational motion. For the function of the involvement of particles the following relation is valid [11, 12]:

$$f_s \equiv \frac{k_s^{\text{p}}}{k_{\text{tur}}} = \left(1 + \Omega_s \sqrt{8\left(1 + \gamma_s^2\right)/\pi} \right)^{-1}.$$

For the average value of the module of the relative velocity of two particles, the following dependence was used [11, 12]:

$$|\Delta \mathbf{v}_{js}^{\text{tur}}| = \left[16 k_{\text{tur}} \left(f_s + f_j - 2\rho_{js} \sqrt{f_j f_s} \right)/3\pi \right]^{0.5},$$

where $\rho_{js} = [1 + 8(\Omega_j^2 f_j + \Omega_s^2 f_s)/\pi]^{-0.5}$. The diffusion coefficients within the framework of the model are estimated by the formula $D_s = 2k_{\text{tur}}T_{\text{E}}/3 + \tau_s k_{\text{B}}T/m_s$.

There exists a complex classification of the regimes of fragmentation of droplets in flows [4]. In calculations, the Weber number was used as a criterion: $\text{We}_s = 2\rho a_s |\mathbf{v}_s - \mathbf{u}|^2/\sigma_{\text{w}}$. The fragmentation was modeled by the doubling scheme: if the local value of the Weber number of the given fraction exceeded the critical one, it was considered that the droplet broke into two identical parts. Thereafter new values of We_s were found, and again they were compared with We_{cr}. When $\text{We}_s \geq \text{We}_{\text{cr}} = 16$, the process was repeated.

In the calculations, the following system of equations of the dynamics of a polydisperse condensate was used:

$$\frac{\partial n_s}{\partial t} + \text{div}\,(\mathbf{v}_s n_s) = \text{div}\,(D_s \nabla n_s) - \frac{1}{2} K_{ss} n_s^2 - n_s \sum_{m=s+1}^{N} n_m K_{sm} (1 - \Phi_{sm}),$$

$$\frac{\partial \rho_s}{\partial t} + \text{div}\,(\mathbf{v}_s \rho_s) = \text{div}\,(D_s \nabla \rho_s) + n_s \dot{m}_s + n_s \sum_{j=1}^{s-1} K_{js} \Phi_{js} \rho_j - \rho_s \sum_{m=s+1}^{N} K_{sm} \Phi_{sm} n_m,$$

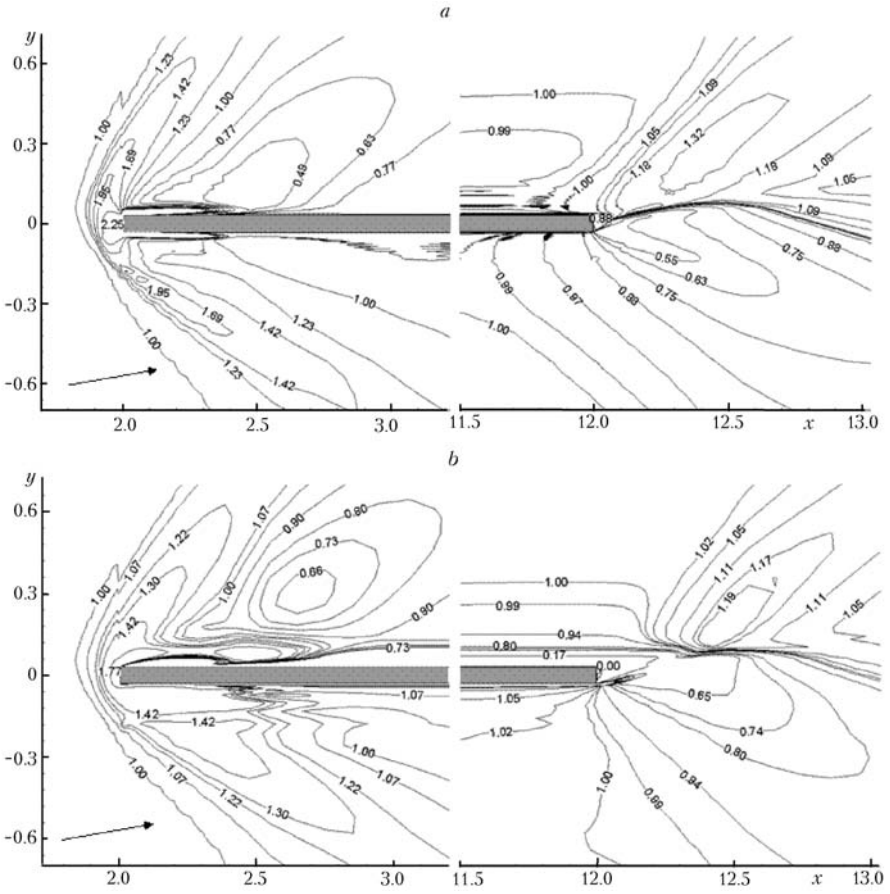

Fig. 1. Isolines of the field of the number density: a) fine fraction (the size "at infinity" is equal to 1 μm); b) large fraction (the size "at infinity" is equal to 10 μm). The arrow shows the direction of the incoming flow. $n\cdot 10^{-6}$, m^{-3}; x, y, m.

$$\frac{\partial \rho_s v_s^{\alpha}}{\partial t} + \operatorname{div}\left(\mathbf{v}_s \rho_s v_s^{\alpha}\right) = \operatorname{div}\left(D_s v_s^{\alpha} \nabla \rho_s\right) + n_s \left(F_s\right)^{\alpha} + n_s v_s^{\alpha} \dot{m}_s$$

$$+ n_s \sum_{j=1}^{s-1} K_{js} \rho_j \left(v_j^{\alpha} - (1 - \Phi_{js})\, v_s^{\alpha}\right) - \rho_s \sum_{m=s+1}^{N} K_{sm} n_m \left(v_s^{\alpha} - (1 - \Phi_{js})\, v_m^{\alpha}\right), \quad \alpha \in \{1, 2\},$$

$$\frac{\partial \rho_s e_s}{\partial t} + \operatorname{div}\left(\mathbf{v}_s \rho_s e_s\right) = \operatorname{div}\left(D_s e_s \nabla \rho_s\right) + n_s q_s + n_s \left(\mathbf{F}_s, \mathbf{v}_s\right) + n_s \left(e_s + L_{\mathrm{v}}\right) \dot{m}_s$$

$$+ n_s \sum_{j=1}^{s-1} K_{js} \rho_j \left(e_j - (1 - \Phi_{js})\, e_s\right) - \rho_s \sum_{m=s+1}^{N} K_{sm} n_m \left(e_s - (1 - \Phi_{sm})\, e_m\right),$$

$$\frac{\partial \rho_{\mathrm{v}}}{\partial t} + \operatorname{div}\left(\mathbf{u} \rho_{\mathrm{v}}\right) = \operatorname{div}\left(D_{\mathrm{v}} \rho_{\Sigma} \nabla \alpha_{\mathrm{v}}\right) - \sum_{s=1}^{N} \dot{m}_s n_s, \quad \rho_{\mathrm{v}} = \alpha_{\mathrm{v}} \rho_{\Sigma}, \quad \rho_{\Sigma} = \rho + \rho_{\mathrm{v}}.$$

Results of Calculations. The computational domain of rectangular form includes one-third of the plate length upstream and approximately two lengths downstream. To decrease the influence of inaccuracies in the simulation of boundary-value conditions on the boundaries of the region, its dimensions were selected so that all the skew compres-

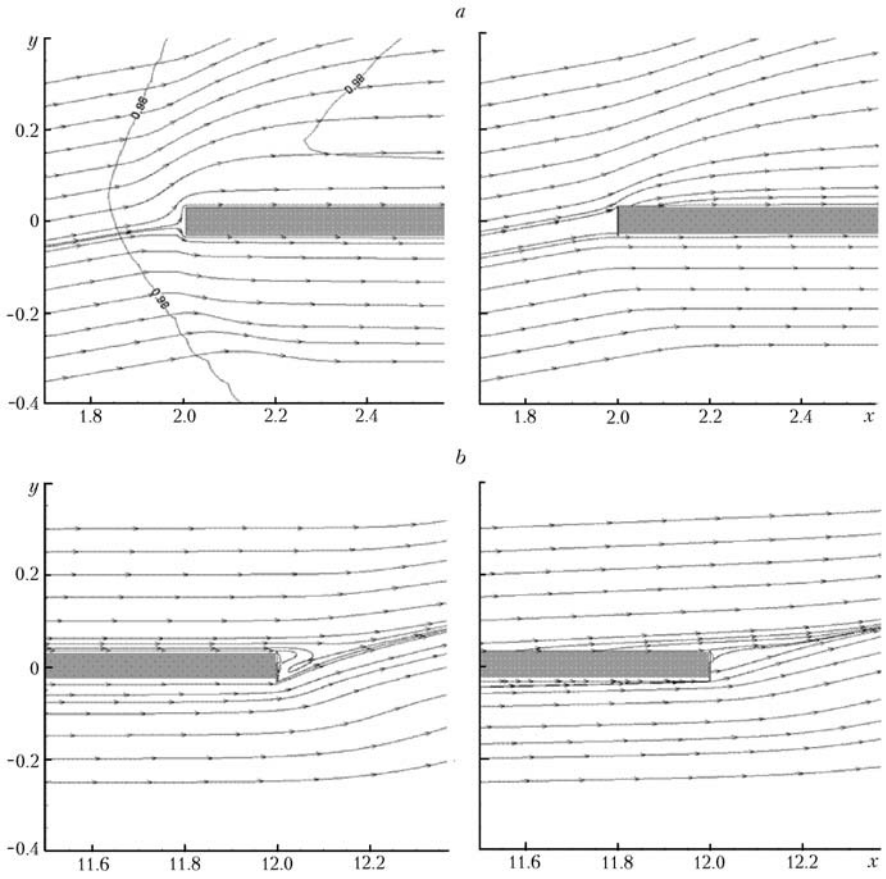

Fig. 2. Trajectories of the particles of the fine (on the left) and large (on the right) fractions of the dispersed phase: a) nose of the plate; b) tail of the plate. *x*, *y*, m.

sion shocks and the fans of rarefaction waves were swept to that part through which the flow escapes. The region was covered by a grid with 533 × 322 rectangular meshes, with finer meshes being located near the body surface. For the gas on the plate, standard boundary conditions of adherence, flow nonexistence, and adiabaticity were used. Calculations were made in two steps: first by the time-dependent technique the flow pattern was obtained in inviscid statement with conditions of flow nonexistence on the body, and then these results were adopted as the initial ones for the equations of the q–ω model which were also solved by the time dependent technique. For satisfactory resolution of the boundary layer, estimates of its thickness were made preliminarily (from the conditions in the incoming flow) within the framework of the problem on a laminar flow past a streamwise infinite flat plate [7]. The fineness of the grid near the body surface was selected so that in the vicinity of its rear edge there were five meshes per estimated boundary layer thickness. The method of large particles made it possible to perform calculations without preliminary singling out the characteristic features of the flow. To find the influence of various input data of the problem, a series of parametric calculations was carried out. Here, it is worthwhile to compare numerical results for various physical situations.

First, we will consider the characteristic features of the behavior of droplets of the different fractions of the condensate within the framework of a fixed regime of flow around particles. Figure 1 presents isolines of number densities of two disperse phase fractions for the regime with $M_\infty = 2$ and an angle of attack of 10^o. At the nose of the plate, changes in the concentrations of the particles of both species are approximately the same as compared to the nonperturbed values (they increase severalfold behind the front of the withdrawn shock wave). In this case, the regions where such changes manifest themselves have a geometrically more compact character for large particles. This can be explained by the higher inertia of the latter due to which their trajectories are distorted only in the zones of more intense changes in the gasdynamic background parameters. Also, the high inertia of large droplets is the reason for the appearance of the local zone of their elevated concentration on the leeward side of the plate at its front. In the rear

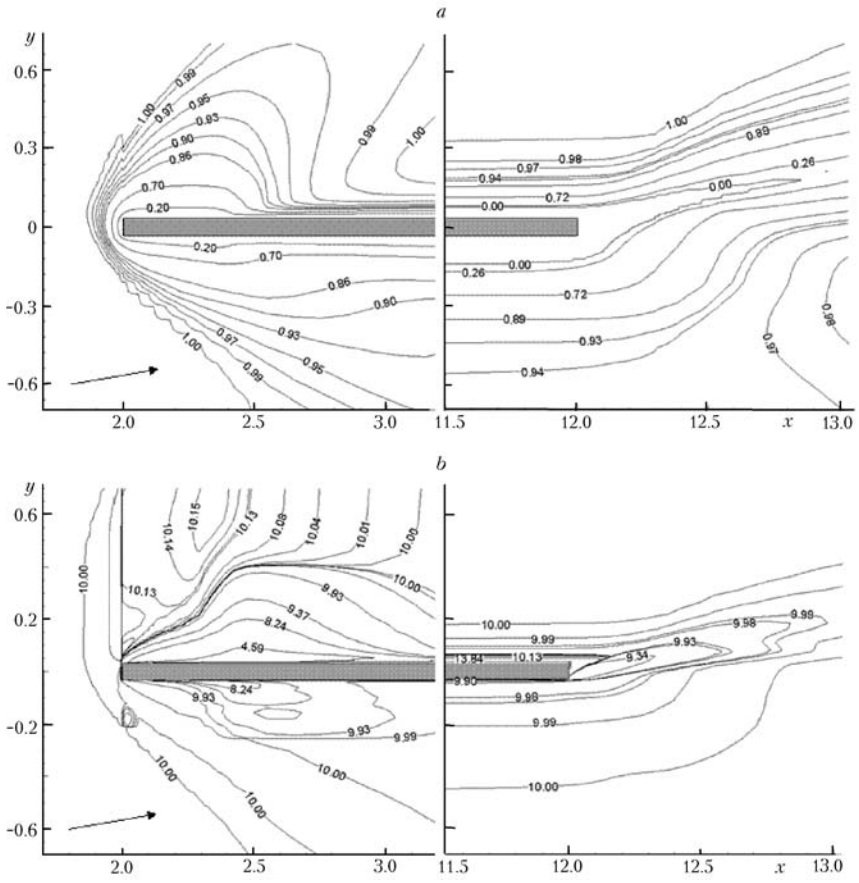

Fig. 3. Isolines of the fields of the radii of droplets: a) fine fraction; b) large one. a_s, μm; x, y, m.

on the leeward side there are noticeably less particles of the large fraction than of fine ones (near the bottom section of the plate there is a zone where large particles are virtually absent). This effect can be attributed to the inertia of large droplets, as a result of which they do not reach the leeward surface of the body exposed to the flow. This conclusion is confirmed by Fig. 2, on which the trajectories of the droplets of two different fractions for one and the same regime are shown. Based on their analysis, we may conclude that the trajectories of the fine fraction practically coincide with the streamlines of the carrying gas. Only a very small portion of the droplets of this radius reach the plate surface, whereas the main portion moves parallel to it. For the large droplets the situation is different. Their trajectories are less distorted than for the fine particles, and on the windward side the trajectories "piercing" this surface are seen. A portion of droplets arriving at the frontal edge of the plate are displaced to the leeward side, move along it, and then separation of their trajectories from the surface occurs. Another reason for the decrease in the number density can be coagulation under the conditions of a strong flow turbulization. The spatial distributions of the radii of the condensate particles of different fractions differ considerably, as is seen from Fig. 3. The fine fraction better relaxes to the flow in velocity and temperature, which explains the practically complete evaporation of its droplets behind the front of the head shock wave. This fact is confirmed by the graphs of Fig. 4, which are vertical sections of the fields of the velocities and temperature of the dispersed phase and gas drawn through the nose of the plate. Also, the role of the coagulation of the particles of this fraction on mutual collisions seems to be important, and it is strengthened as a result of the involvement of particles in the developed turbulent motion of the gas accompanied by an increase in their radius (see Fig. 3b). The rate of change in the temperature of a particle is inversely proportional to its radius; therefore, the particles of the fine fraction in the wall region of the rear part of the plate practically entirely evaporate in a hot boundary layer. As a consequence, a zone free of them is formed and it propagates downstream approximately over the tenth part of the length of the body exposed to the flow. In the model of coagulation adopted in calculations, growth of droplets of the given species is possible during their collisions with finer ones. The frequency of

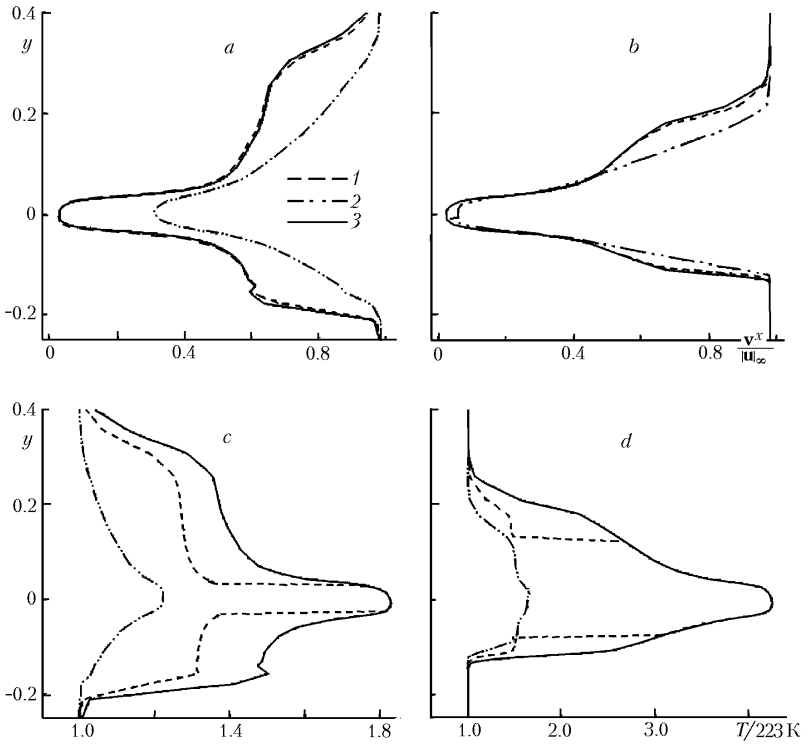

Fig. 4. Dependence of the horizontal components of the velocity (a, b) and temperatures (c, d) of the dispersed phase and gas on the vertical coordinate at the frontal part of the plate: a, c) M = 2, b, d) 4; 1) fraction with the radius "at infinity" of 1 μm; 2) 10 μm; 3) carrying gas. *y*, m.

collisions of particles is directly proportional to the rate of pulsations. In the zone considered the rate of pulsations increases by several orders of magnitude in comparison with the background value. As a result, in Fig. 3 we observe an increase in the radius of the particles of the large fraction by tens of percent on the leeward side of the rear part. The graphs of Fig. 4a and b allow one to compare the degrees of relaxation in velocity to the carrying gas particles of two different fractions in different regimes of exposure to the flow. On the whole we note that the finer the particles, the better they "adapt" to the flow. The smaller differences of the horizontal velocities of droplets from the gas velocity for the regime with $M_\infty = 4$ as compared to the regime with $M_\infty = 2$ is attributable to the preliminary fragmentation of particles in the head shock wave. However, there may not be complete relaxation, as is seen for the regime with $M_\infty = 2$, where the difference attains about 30% for the large fraction. In Fig. 4c and d the temperatures of the fractions and gas in the same section of the computational domain are compared. It is evident that the temperature-related relaxation manifests itself less than the velocity-related, which is due to the large characteristic time of the processes of heat transfer. The difference of temperatures of the large fraction particles and gas can amount to more than 50%.

It is of interest to continue the comparison of the results of calculations of a two-phase flow past a plate at different data "at infinity." Figures 5 and 6 present the isolines of the fields of numerical concentration and radii of droplets of two fractions of condensate for the regime with $M_\infty = 4$. On the whole we may note the same characteristic features as in the previous case, although we may point to a certain specific feature. The zone of complete evaporation of the fine fraction becomes thicker near the body surface: it begins directly behind the head shock wave front and ends approximately at a distance equal to one-fifth of the plate length down the flow from the bottom section. Here the heating of the carrying gas turns to be higher than in the previous case in the flow inhomogeneities and in the boundary layer, which leads to an increase in the heat fluxes to droplets, their more intense heating, and rapid evaporation. Out of the three available fractions (fine, intermediate, and large) this effect is most evident for the finest one. In contrast to the previous regime, in the front part of the plate, zones with a characteristic dimension of the order of several body thicknesses are observed in which the number density of both fractions increases considerably

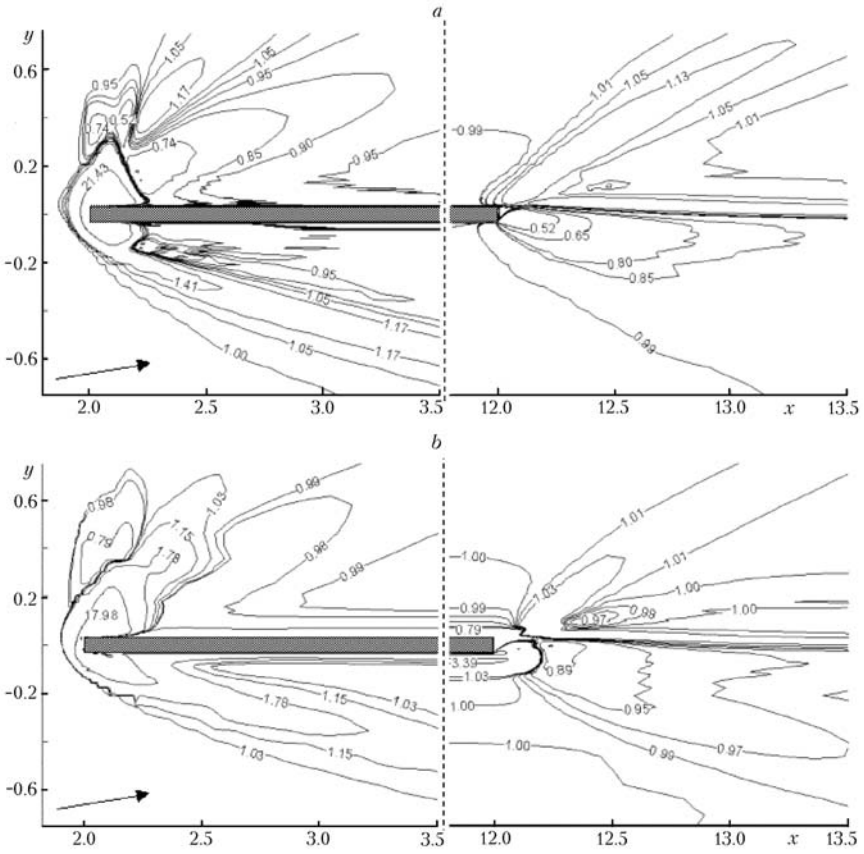

Fig. 5. Isolines of the field of the number density: a) fine fraction; b) large fraction. Regime with M_∞ = 4, angle of attack 10°. The arrow shows the direction of the incoming flow. $n \cdot 10^{-6}$, m^{-3}; x, y, m.

(approximately ten times), whereas the radii decrease by an order of magnitude. This effect is explained by the influence of the fragmentation of droplets when they pass through the departed shock wave, which did not occur at a lower Mach number of the incoming flow.

Figure 7 illustrates the results of calculations of the large-fraction droplet radius in the vicinity of the frontal edge of the body exposed to a flow when allowance is made for the processes of coagulation/fragmentation and with neglect of the above effects. Substantial differences in the spatial location of the lines of the level and a more compact character of the regions of evident changes in the radius in the first case can be noted. There is a general tendency towards a decrease in the radii of droplets of all fractions in the near-surface zone as a result of evaporation in the heated boundary layer. Allowance for coagulation somewhat retards this process: As a result of the coalescence of droplets on mutual collisions, the decreases in their radii near the plate is manifested less than when only phase transitions are taken into account. The curves of Fig. 8a and b show that because of the coagulation the fine fraction comes into equilibrium with respect to temperature with the carrying gas much closer to the surface exposed to the flow (the temperature slip in the region of difference attains about 30%), whereas the droplets of the intermediate fraction reach it at a temperature 1.5 times lower. As seen from Fig. 8c and d, in calculations with allowance for coalescence-caused coagulation from the windward side of the plate the number density of the fine fraction undergoes smaller changes (by a factor of 1.5–2) as compared to the case where these phenomena are ignored and where the increase in the number density is due only to the specific location of the trajectories of particles. From the leeward side, the droplets of the intermediate fraction are larger near the plate surface than in the coagulation-free case. As a result of the higher inertia and emission of fragments appearing on fragmentation of the large fraction, the number density exceeds several times the values obtained with no regard for coagulation/fragmentation. In the latter case, at a distance of the order of the plate thickness the droplets come into temperature equilibrium with the gas because of the substan-

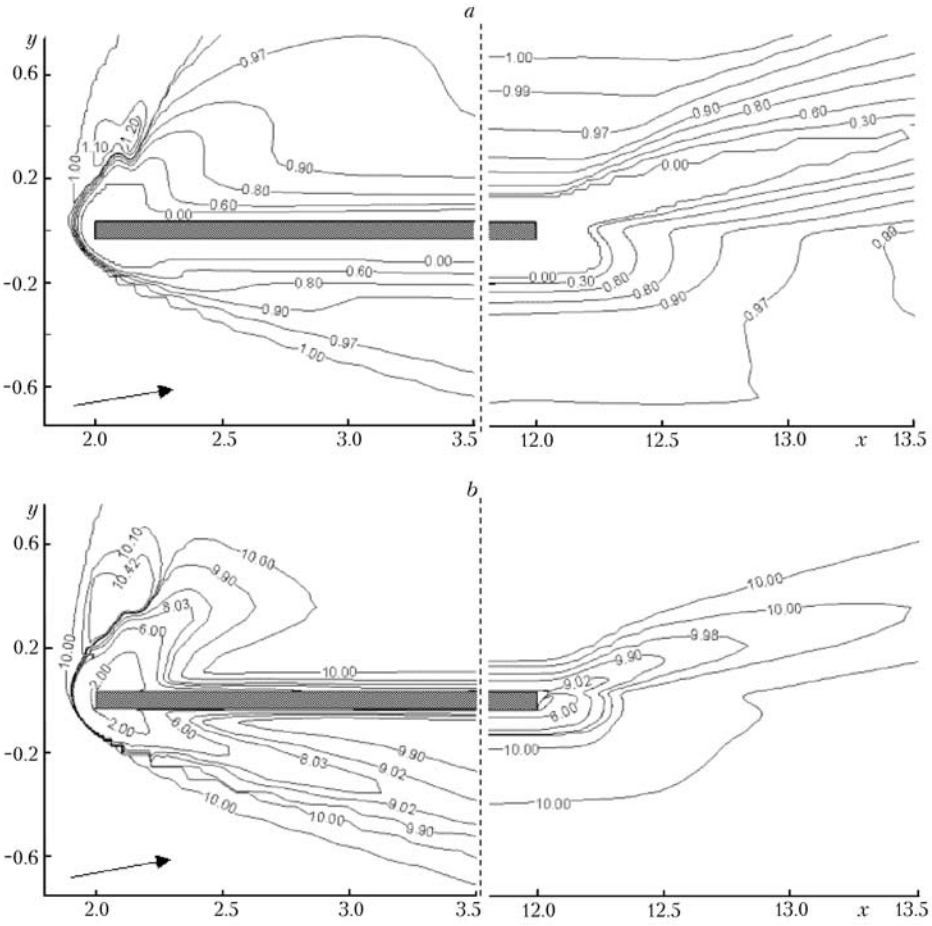

Fig. 6. Isolines of the fields of the radii of droplets (μm): a) fine fraction; b) large fraction. The inlet data are same as in Fig. 5. *x*, *y*, m.

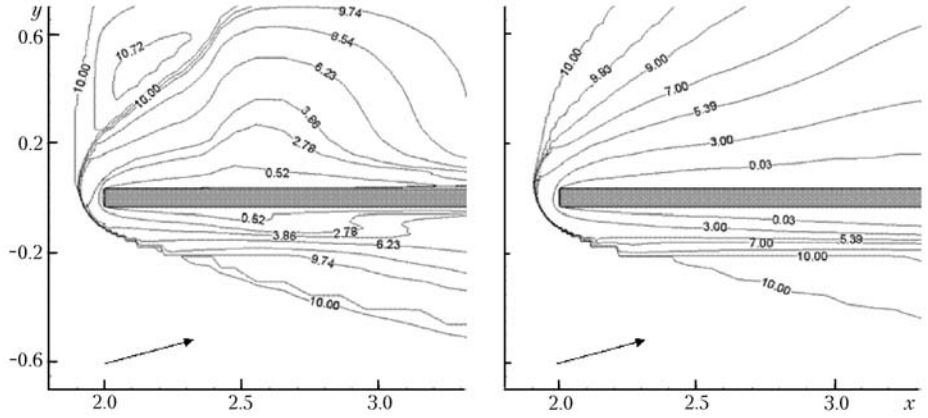

Fig. 7. Isolines of the field of the radius of the large fraction (the size "at infinity" is equal to 10 μm) of the dispersed phase with allowance for coagulation/fragmentation (on the left) and with no regard for these processes (on the right). The regime with $M_\infty = 4$, angle of attack 15°, $n_\infty = 10^6$ m^{-3}, $T_\infty = 223$ K. The arrow indicates the direction of the incoming flow. *x*, *y*, m.

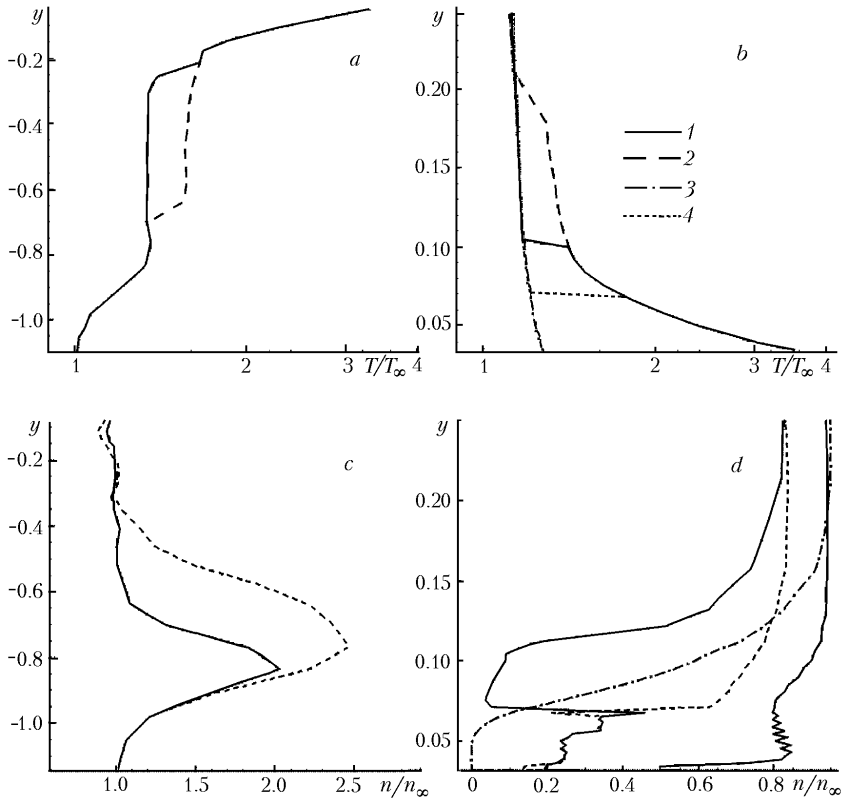

Fig. 8. Dependence of the temperature (a, b) and concentration (c, d) of the dispersed phase on the vertical coordinate for the windward (a, c) and leeward (b, d) sides at the middle of the plate: 1) fine fraction with regard for coagulation/fragmentation; 2) same with no regard for them; 3) intermediate fraction with regard; 4) same with no regard. Input data are same as for Fig. 7. y, m.

tial decrease in their radius due to evaporation. When coagulation is taken into account, the decrease in the radius is less evident; therefore, the temperature relaxation to the flow is not observed in the particles of the given fraction. On the basis of these results, we may emphasize the important role of the processes of coagulation of droplets in studying the transformation of their mass spectrum in a multiphase flow past a flying vehicle.

CONCLUSIONS

1. With the aid of the numerical codes developed by the present author, the verification of a synthetic physicomathematical model of the evolution of a polydisperse two-phase flow is carried out. Methodical calculations of a supersonic two-phase polydisperse flow past a flat plate have been performed. The evolution of different fractions of a condensate, as well as the influence of the incoming flow Mach number on the spatial distribution of the basic parameters of dispersed substance, is investigated.

2. The influence of coagulation/fragmentation of droplets on the transformation of their mass spectrum has been established, and the importance of the allowance for these effects is shown.

This work has been carried out with financial support from the Russian Fundamental Research Foundation, grants 08-01-00540-a and 07-08-00732.

NOTATION

a, radius, m; c_w, specific heat of water, J/(kg·K); C_D, coefficient of aerodynamic resistance; D_s, coefficient of diffusion of particles of fraction s, m^2/sec; $e_s = c_w T_s + |\mathbf{v}_s|^2/2$, total specific energy, m^2/sec^2; f_s, function of the in-

volvement of particles of fraction s into pulsational motion; K_B, Boltzmann constant, J/K; $K_{js} = \pi(a_j + a_s)^2 \left| \Delta \mathbf{v}_{js} \right|$, kernel of the collisions of particles of the jth and sth fractions, m^3/sec; k_s^p, specific energy of pulsational motion; m^2/sec^2; k_{tur}, specific energy of turbulent pulsations, m^2/sec^2; L_v, specific heat of water evaporation, J/kg; M, Mach number; $\dot{m}_s$, rate of change in the mass of a particle in phase transition, kg/sec; $m_s = 4\pi a_s^3 \rho_w/3$, mass, kg; n_s, local number density, m^{-3}; Pr, Prandtl number; q_s, heat flux to the particle surface, J/sec; T, temperature, K; $T_E \sim k_{tur}/\varepsilon_{tur}$, Euler temporal macroscale of turbulence, sec; T_s, mean-bulk temperature, K; t, time, sec; $\mathbf{u}$, averaged velocity, m/sec; $\mathbf{v}_s(v_s^1, v_s^2)$, vector of the velocity of transactional motion, m/sec; x, y, coordinates, m; γ, adiabatic index; $\gamma_s = \left| \mathbf{v}_s - \mathbf{u} \right| / \sqrt{2k_{tur}}$, parameter of slipping; ε_{tur}, rate of dissipation of the average specific energy of turbulent pulsations, m^2/sec^3; $\mu_m(T)$, coefficient of molecular dynamic viscosity, kg/(m·sec); ρ, mass concentration (density), kg/m^3; ρ_s, local mass concentration, kg/m^{-3}; ρ_v, mass concentration of steam in a carrying flow, kg/m^3; ρ_w, density of water, kg/m^3; σ_w, coefficient of the surface tension of water, N/m; $\tau_s = 2a_s^2 \rho_w/\mu_m(T)$, time of dynamic (Stokesian) velocity relaxation of a droplet, sec; Φ_{js}, coefficient of coagulation/fragmentation; $\Omega_s = \tau_s/T_E$, inertia parameter; ω, exponent in the law of the temperature dependence of the dynamic viscosity of gas. Subscripts and superscripts: c, continuous; cr, critical; j, m, s, fractions; m, molecular; p, particle; r, rarefied; rand, random velocity component; tur, turbulent; v, vapor; w, water.

REFERENCES

1. M. M. Gilinskii and A. L. Stasenko, *Supersonic Gas Disperse Jets* [in Russian], Mashinostroenie, Moscow (1990).
2. A. L. Stasenko, *Physical Mechanics of Multiphase Flows* [in Russian], Izd. MFTI, Moscow (2004).
3. I. M. Vasenin, V. A. Arkhipov, V. G. Butov, A. A. Glazunov, and V. F. Trofimov, *Gas Dynamics of Two-Phase Flows in Nozzles* [in Russian], Izd. Tomsk Univ., Tomsk (1986).
4. L. E. Sternin and A. A. Shraiber, *Multiphase Particle-Laden Flows* [in Russian], Mashinostroenie, Moscow (1994).
5. T. J. Coakley, Turbulence modeling methods for the compressible Navier–Stokes equations, *AIAA-Paper*, No. 83-1693 (1983).
6. O. M. Belotserkovskii and Yu. M. Davydov, *Method of Large Particles in Gas Dynamics* [in Russian], Nauka, Moscow (1982).
7. L. G. Loitsyanskii, *Mechanics of Liquids and Gases* [in Russian], Nauka, Moscow (1987).
8. M. N. Kogan, *Rarefied Gas Dynamics* [in Russian], Nauka, Moscow (1968).
9. S. E. Herner, *Fluid-Dynamic Drag*, Published by the author (1958).
10. I. V. Derevich, Collisions of particles in a turbulent flow, *Izv. Ross. Akad. Nauk*, *Mekh. Zhidk. Gaza*, No. 2, 104 (1996).
11. I. V. Derevich, Statistical modeling of particles relative motion in a turbulent gas flow, *Int. J. Heat Mass Transfer*, **49**, 4290–4304 (2006).
12. I. V. Derevich, Coagulation kernel of particles in a turbulent gas flow, *Int. J. Heat Mass Transfer*, **50**, 1368–1387 (2007).
13. Y. H. Pao, Structure of turbulent velocity and scalar fields at large wave numbers, *Phys. Fluids*, **8**, 1063–1075 (1965).